

# Magnetic Flux Periodic Response of Nano-perforated Ultrathin Superconducting Films

M. D. Stewart, Jr., Zhenyi Long, James M. Valles, Jr.  
*Department of Physics, Brown University, Providence, RI 02906*

Aijun Yin and J. M. Xu  
*Division of Engineering, Brown University, Providence, RI 02906*  
 (Dated: 5th October 2018)

We have patterned a hexagonal array of nano-scale holes into a series of ultrathin, superconducting Bi/Sb films with transition temperatures  $2.65 \text{ K} < T_{co} < 5 \text{ K}$ . These regular perforations give the films a phase-sensitive periodic response to an applied magnetic field. By measuring this response in their resistive transitions,  $R(T)$ , we are able to distinguish regimes in which fluctuations of the amplitude, both the amplitude and phase, and the phase of the superconducting order parameter dominate the transport. The portion of  $R(T)$  dominated by amplitude fluctuations is larger in lower  $T_{co}$  films and thus, grows with proximity to the superconductor to insulator transition.

The superconductors originally considered by BCS exhibited spectacularly sharp transitions from a finite resistance to zero resistance as a function of temperature [1]. Fluctuation effects were negligible. Presently, a great deal of attention focuses on low superfluid density superconductors for which fluctuations strongly influence and substantially broaden their phase transitions. These include the high temperature superconductors [2], and in particular, their underdoped versions [3, 4, 5], and ultrathin superconducting films near the superconductor to insulator transition (SIT) [6, 7, 8, 9, 10]. For the latter, resistive transitions,  $R(T)$ , can develop widths comparable to or greater than the apparent mean field transition temperature,  $T_{c0}$  [11].

To discuss the effects of fluctuations on the  $R(T)$  it is helpful to consider the two component superconductor order parameter  $\psi = |\psi_0|e^{i\phi}$ . In bulk elemental superconductors, the sharp  $R(T)$  reflect the near simultaneous appearance of a finite amplitude,  $|\psi_0|$ , and long range coherence of the phase,  $\phi$ . In low superfluid density superconductors, however, the amplitude first forms at high temperatures and phase coherence develops at lower temperatures [2, 12, 13, 14]. High on a transition quasiparticles transiently form Cooper pairs, which enhances the quasiparticle or fermionic contribution to the conductivity,  $\sigma_f$ . These pair or amplitude fluctuations give rise to the initial drop in  $R(T)$  [15]. At very low values of  $R$ , a substantial Cooper pair density exists and the conductivity of these bosons,  $\sigma_b$ , controls  $R(T)$ .  $\sigma_b$  is limited by the motion of vortices which causes fluctuations in the phase of the cooper pair condensate. In between, a two fluid model may best describe the transport [7].

Physical interpretations of the  $R(T)$  in high sheet resistance films especially those near the SIT relies heavily on distinguishing the amplitude and phase fluctuation dominated regimes [3, 4, 5, 6]. Most often, explicit models for  $\sigma_f(T)$  and  $\sigma_b(T)$  do not exist as a guide and qualitative arguments must prevail. In this paper we present the magnetic flux response of the  $R(T)$  of very low superfluid density (high sheet resistance) [11, 16] films patterned with a nanoscale array of holes. We use the quality of the flux response at different points along their transitions to determine the presence of

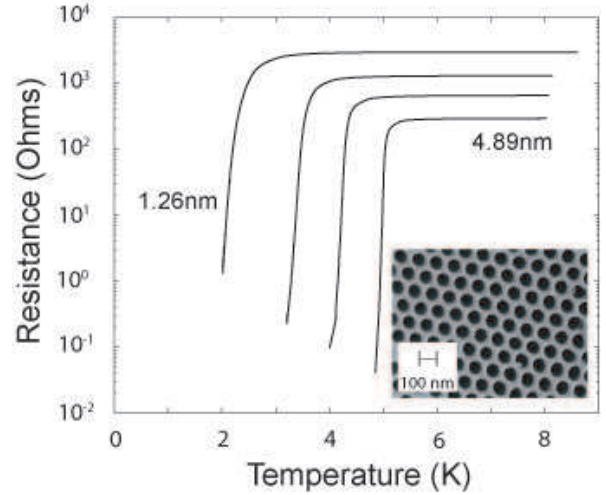


Figure 1: Superconducting transitions for a perforated film. Inset shows an SEM image of one of the substrates used in these experiments. The hole lattice constant is  $a = 100 \text{ nm}$  and  $R_{hole} = 33 \text{ nm}$ .

well-defined vortices [17] and thus provide insight into where the amplitude fluctuation dominated transport gives over to phase fluctuation dominated transport on an  $R(T)$ . In addition, we propose that this method can be used to directly detect the existence of vortices in settings where their presence has been contentious [8].

As a consequence of phase coherence, magnetic field periodic behavior is expected in films with multiply connected periodic geometries (see inset of Fig. 1) [18, 19]. For example, the resistive transitions of thick Nb films [20] on nanopore arrays and thick Al films with much larger lattice and hole dimensions [21] oscillate in temperature while maintaining their shape in an applied magnetic field. For holes separated by segments on the order of  $\xi_0$  or less [20]

$$\frac{\Delta T_c}{T_{c0}} = - \left( \frac{\xi_0}{a} \right)^2 \left( \frac{1}{4} - \left( \frac{\phi}{\phi_0} - n - \frac{1}{2} \right)^2 \right) \quad (1)$$

where  $\Delta T_c$  is the shift in the transition,  $\xi_0$  is the (dirty) co-

herence length,  $a$  is the hole to hole spacing [22],  $n$  is an integer, and  $\phi$  is the applied magnetic flux.  $\phi_0 = H_m \left( \frac{\sqrt{3}}{2} a^2 \right)$  is the magnetic flux corresponding to having one flux quantum per unit cell and defines the unit cell matching field,  $H_M$ . Eq. 1 is derived within the context of mean field theory, or in the absence of appreciable fluctuations of the superconducting order parameter and without considering vortex motion. Therefore, the physical picture which leads to Eq. 1 is that of immobile vortices which penetrate the film through the array of holes. These vortices generate screening currents which, at  $H = nH_M$ , nearly cancel in the interior of the film so that  $\Delta T_c \simeq 0$ . At incommensurate fields the screening currents give rise to pair breaking and thus, a reduction in  $T_c$ . The microscopic picture described by Eq. 1 is the familiar Little-Parks physics.

Eq. 1 accounts well for the flux periodic behavior of thick Nb films [20]. Our data, however, show that this physical picture is not valid for ultrathin high sheet resistance films with low superfluid density. Amplitude fluctuations prevent the formation of screening currents as described above when the fraction of the normal state resistance  $r = R/R_N \gtrsim 0.5$ . In addition, as  $r$  decreases ( $r \lesssim 0.15$ ) and screening currents appear, the films' susceptibility to thermal fluctuations allows activated vortex motion to dominate the transition. Our data also indicate that the region of the transition dominated by amplitude fluctuations grows with decreasing  $T_{c0}$  and hence increasing proximity to the SIT.

Our experiments were conducted on homogeneous quench condensed Bi/Sb films similar to those employed in previous studies of the SIT and Thermally Activated Flux Flow (TAFF) [11]. These films have very low superfluid density because they are thin and disordered [11, 16]. Two films were made simultaneously for each experiment. One film was deposited on a fire-polished glass substrate while the other was deposited on a nano-perforated Anodic Aluminum Oxide (AAO) substrate (see the inset of Fig. 1). The latter assumed the honeycomb geometry of the substrate. The preparation of the AAO substrates can be found elsewhere in the literature [23, 24, 25, 26]. Those used in these experiments had a hole lattice constant,  $a$ , of 100 nm and a hole radius,  $R_{hole} = 33$  nm. Both substrates were precoated with 50 nm of thermally evaporated Ge (in an attempt to smooth the small surface roughness of the AAO substrate) before Au contact pads were deposited at room temperature. Subsequently both substrates were mounted in our cryostat where homogeneous Bi films are fabricated at  $T = 8$  K by first evaporating a thin film of Sb ( $< 1$  nm, which ensures the films' homogeneous morphology) and then depositing the desired thicknesses of Bi through sequential depositions. In this way, a series of Bi films were fabricated without breaking vacuum or warming.

The  $R(T)$  were measured using standard four-terminal, low-frequency ac techniques and acquired in the regime of applied currents where the films exhibit an ohmic response. Nonlinearities associated with the phase transition to the zero resistance state, which are expected at lower temperatures and

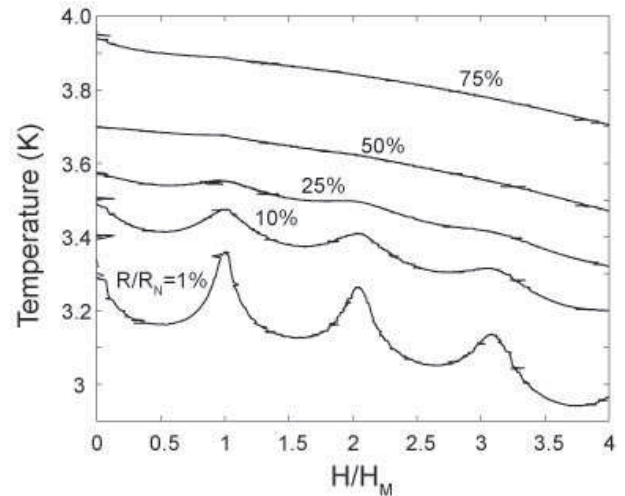


Figure 2: Iso-dissipative measurements of temperature vs magnetic field (normalized by the matching field) for a representative perforated film with  $d_{Bi} = 1.90$  nm,  $T_{c0} = 3.70$  K,  $r_{hole} = 33$  nm, and hole spacing  $a = 100$  nm. Inset shows the corresponding superconducting transition with the arrows indicating the value of  $R/R_N$  where the curves in the main panel were taken. Eq. 1 predicts that each curve should exhibit the same magnitude oscillation of  $\approx 0.01$  K.

have been observed in some wire arrays do not appear in this experiment's range [27, 28, 29]. The normal state resistances,  $R_N$ , of neighboring film regions were compared to assess film homogeneity and found to agree to  $< 7\%$ . Magnetic fields were applied perpendicular to the planes of the films. Our thermometry consists of a calibrated carbon glass resistor which has a negligible magnetoresistance in the range of fields used in these experiments.

Data from a series of four superconducting films with  $T_{c0}$  ranging from 2.65 to 5 K and normal state resistances,  $R_N = R(8K)$ , ranging from 3.3 k $\Omega$  to 300  $\Omega$  are shown in Fig. 1. The reference film exhibits the same range of  $T_{c0}$  and a similar increase in the widths of its transitions with decreasing  $T_{c0}$ . The latter characteristic has been ascribed to a growing fluctuation dominated regime [11]. The systematic reduction in  $T_{c0}$  is believed to result from disorder enhanced Coulomb repulsion effects that grow with increasing  $R_N$  and possibly drive the SIT [30, 31].

Despite the breadth of the superconducting transitions they do oscillate with increasing magnetic field. The amplitude of the oscillations, however, depends strongly on the reduced resistances,  $R(T)/R_N$ , at which they are measured. That is, unlike thicker films the shape of the transitions change in field [20, 21]. Figure 2 shows a typical series of isodissipative (i.e. fixed  $r$ ) measurements of  $\Delta T$  [32]. ( $R_N$  does not change in this range of applied fields.) The lower  $r$  curves exhibit oscillations that diminish in size with increasing field and are superimposed on a nearly quadratic background. The peaks in the data appear at  $H = nH_m = n(2145 \pm 50)$  Gauss where  $n$  is an integer.  $H_M$  corresponds closely to the calcu-

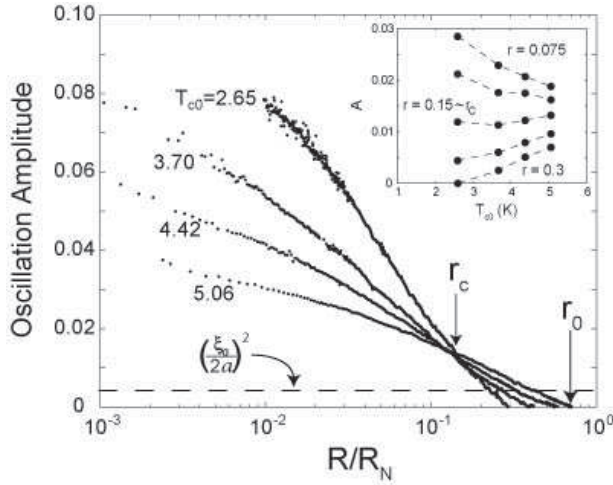


Figure 3: Normalized amplitude of the first temperature oscillation as a function of fractional resistance for 4 perforated films with  $2.65 < T_{c0} < 5.06\text{K}$ ,  $R_{hole} = 33\text{nm}$ , and  $a = 100\text{nm}$ . Inset shows the unexpected behavior of the  $A(r)$  with  $T_{c0}$  near  $r_c$ .

lated value for one flux quantum per unit cell of the hole array (see [22]). Thus, these oscillations result from the collective response of the hole array rather than from the responses of single holes [33]. A feature of particular interest is that the peak amplitudes are larger at lower  $r$ .

We characterize the flux periodic response using a normalized oscillation amplitude,  $A$ , for the first oscillation:

$$A = \frac{T(r, 0) + T(r, H_M)}{2T_{c0}} - \frac{T(r, H_M/2)}{T_{c0}}, \quad (2)$$

Each solid curve of  $A$  as a function of  $r$  shown in Fig. 3 was calculated using individual measurements of  $R(T)$  at 0,  $H_M/2$ , and  $H_M$ . The dashed curve represents the mean field oscillation amplitude,  $A_{MF} = (\xi_0/2a)^2$ , derived from Eq. 1.  $\xi_0 \simeq 10\text{ nm}$  represents the average value for these films as determined from measurements of the upper critical fields of the reference films. It varied by 20% over this range of  $T_{c0}$ .

The oscillation amplitudes exhibit a rich dependence on  $r$  and  $T_{c0}$ , unlike the constant mean field prediction. For all  $T_{c0}$ ,  $A$  grows nearly logarithmically from zero with decreasing  $r$  with a dependence that is stronger for the films with lower  $T_{c0}$ . For  $r \ll 1$ , the oscillations surpass 10 times the mean field result. The  $r$  at which oscillations first appear,  $r_0$ , is well defined and is lower for lower  $T_{c0}$ . Interestingly, the  $A(r)$  for different  $T_{c0}$  cross in the vicinity of a single point near  $r = r_c \simeq 0.15$ . The existence of this crossing point is supported by data on another hole size. Its significance is brought out partially by the inset in Fig. 3, which shows how  $A$  depends on  $T_{c0}$  at fixed values of  $r$ .  $r_c$  delineates the portions of the  $R(T)$  in which  $A$  increases or decreases with the primary energy scale characterizing the transition,  $T_{c0}$ .

Accounting for the very large  $A$  at low  $r$  and the vanishing of  $A$  for  $r \simeq \frac{1}{2}$  clearly requires consideration of the effects of fluctuations [34]. Unfortunately, detailed theoretical pre-

dictions for the  $R(T)$  do not exist. Our identification of two scales in the data,  $r_0$  and  $r_c$ , however, provide a useful guide for the discussion. As we emphasize below, the two scales define points on the transitions at which the dissipative processes and character of the fluctuation effects qualitatively change.

Insight into the large amplitude of the oscillations at  $r < r_c$  comes from investigating the tails of the superconducting transitions in magnetic field. Figure 4 shows Arrhenius plots of the  $R(T)$  collected at  $H = 0$ ,  $H_M/2$ , and  $H_M$  for two films with different  $T_{c0}$ . The tails of the  $R(T)$  follow

$$R(T) = R_0 e^{(-T_0/T)}, \quad (3)$$

which is the signature of Thermally Activated Flux Flow (TAFF). The energy barrier,  $T_0$ , is lower by more than a factor of 2 at  $H = H_M/2$  than at  $H = H_M$ . This nonmonotonic variation in  $T_0$  gives rise to the  $\Delta T$  oscillations that continuously grow as  $r \rightarrow 0$ . At  $H = H_M$  the vortices come into registry with the holes and thus their lattice is made stiff against thermally activated flux flow. At half integer values of  $H/H_M$ , vortices cannot come into registry with the holes and

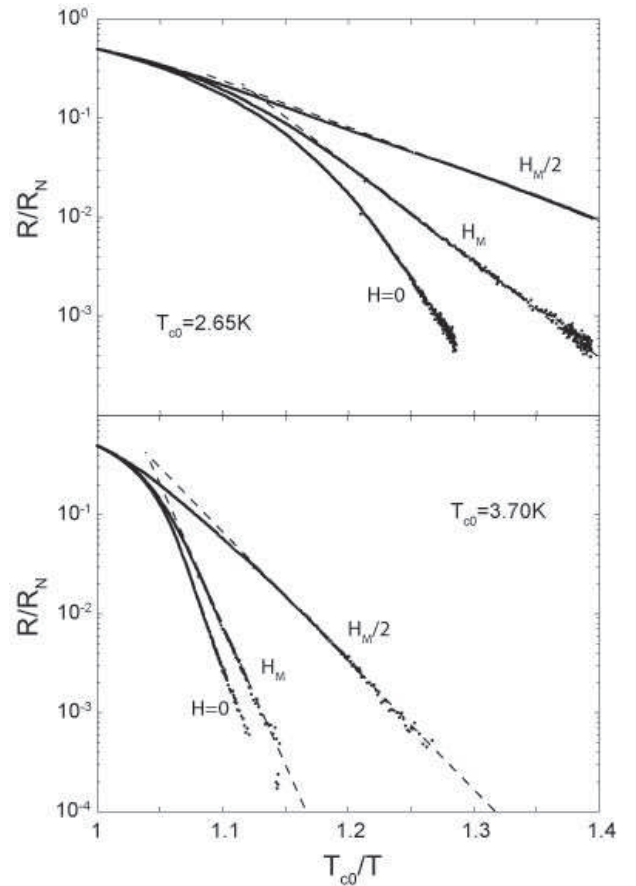


Figure 4: Arrhenius plots for the perforated film with  $R_{hole} = 33\text{nm}$ .  $T_{c0} = 2.65\text{K}$  (top) and  $T_{c0} = 3.7\text{K}$  (bottom). The slope of the curve characterizes the energy barrier against vortex motion in the film. The barrier in the perforated film is non-monotonic with field. Dashed lines are fits to Eq. 3.

simultaneously form a stable lattice. Consequently, the activation energy is substantially lower at incommensurate fields. That lower  $T_{c0}$  films have larger oscillation amplitudes in this regime results from the difference in the activation barriers for different  $T_{c0}$  films as seen in Fig. 4. Even on a normalized temperature scale, the lower  $T_{c0}$  film has broader transitions than the higher  $T_{c0}$  film. Correspondingly, the activation energy increases faster than linearly with  $T_{c0}$ . This behavior is consistent with the condensation energy dictating the activation energy scale. A more detailed discussion of the TAFF behavior will appear in future work.

Moving up the transition to  $r > r_c$  (Fig. 3), the oscillation amplitudes wane and eventually go to zero. The behavior as  $r \rightarrow r_0$  can be attributed to enhanced vortex mobility that causes them to lose registry with the holes. Nearer  $T_{c0}$  the shrinkage of the order parameter makes the barrier to interhole vortex motion smaller and the likelihood of amplitude fluctuations greater. Given that the constrictions in the film are quasi-1d (a few  $\xi_o$  across) both of these effects will enhance interhole vortex motion. These effects are more pronounced in lower  $T_{c0}$  films since the condensation energy, which is proportional to  $T_{c0}$ , governs their strength. Consequently,  $A$  is lower in lower  $T_{c0}$  films. As  $r$  exceeds  $r_0$ , all evidence of well defined vortices that could be pinned by holes and give rise to a periodic response disappears. This last regime can be characterized by amplitude fluctuations that become so strong that they destroy fluxoid quantization altogether.

Thus, even in the absence of a detailed model of  $R(T)$  which accounts for fluctuations in these films, we can identify three distinct fluctuation regimes defined by  $r_c$  and  $r_0$ . For  $r < r_c$ , thermally activated flux motion causes phase fluctuations. In the intermediate regime,  $r_0 > r > r_c$ , the vortex mobility is augmented by strong amplitude fluctuations. And finally, for  $r_0 < r < 1$  amplitude fluctuations dominate and vortices do not exist.

The decrease of  $r_0$  with  $T_{c0}$  implies that the size of the amplitude fluctuation dominated regime increases closer to the SIT [11]. This trend can be attributed to the growth of both the quantum critical regime of the SIT [35] and the classical critical regime [36] as  $R_N$  increases.  $R_N \simeq R_c/2$  for the lowest  $T_{c0}$  film in the series. It suggests that the fermionic degrees of freedom strongly influence the approach to the SIT in uniform films. Experiments on lower  $T_{c0}$ , higher  $R_N$  films will provide insight into whether bosonic (vortices) or fermionic degrees of freedom dominate the SIT.

We propose that techniques similar to those applied here may be useful for detecting the existence of vortices in other unconventional situations. For example, evidence from Nernst Effect [3] and magnetoresistance [4] measurements suggests the presence of vortices well above  $T_c$  in under doped high  $T_c$  compounds. Underdoped films patterned with an ordered array of pinning centers (e.g. holes or magnetic impurities) should exhibit flux periodic behavior according to our results. Similar arrangements [8] could test the proposal that there are vortices on the insulating side of the superconductor to insulator transition.

In summary, we have quenched condensed nano-perforated, homogeneously disordered Bi films. The regular perforations induce a phase-sensitive periodic response to an applied magnetic flux and thus provides a probe capable of distinguishing between the two types of superconducting fluctuations. In these low superfluid density films, we have found that the strength of this response crosses over between regions of the  $R(T)$  dominated by fluctuations in the amplitude,  $|\psi_0|$ , of the superconducting order parameter to that dominated by fluctuations in the phase,  $\phi$ . In addition, as  $T_{c0}$  is lowered and the system approaches the quantum critical point of the SIT, the region of the  $R(T)$  dominated by amplitude fluctuations grows.

This work has been supported by the NSF through DMR-0203608, AFRL, and ONR. We acknowledge helpful conversations with N. Daniilidis.

- 
- [1] J. Bardeen, L. N. Cooper, and J. R. Schrieffer, Phys. Rev. **108**, 1175 (1957).
  - [2] V. J. Emery and S. A. Kivelson, Nature **374**, 434 (1995).
  - [3] Z. A. Xu, N. P. Ong, Y. Wang, T. Kakeshita, and S. Uchida, Nature **406**, 486 (2000).
  - [4] V. Sandu, E. Cimpoiasu, T. Katuwal, S. Li, M. B. Maple, and C. C. Almasan, Phys. Rev. Lett. **93**, 177005 (2004).
  - [5] V. N. Zavaritsky and A. S. Alexandrov, Phys. Rev. B **71**, 012502 (2005).
  - [6] A. F. Hebard and M. A. Paalanen, Phys. Rev. Lett. **65**, 927 (1990).
  - [7] A. Yazdani and A. Kapitulnik, Phys. Rev. Lett. **74**, 3037 (1995).
  - [8] N. Marković, A. M. Mack, G. Martinez-Arizala, C. Christiansen, and A. M. Goldman, Phys. Rev. Lett. **81**, 701 (1998).
  - [9] L. Merchant, J. Ostrick, R. P. Barber, Jr., and R. C. Dynes, Phys. Rev. B **63**, 134508 (2001).
  - [10] G. Sambandamurthy, L. W. Engel, A. Johansson, and D. Shahr, Phys. Rev. Lett. **92**, 107005 (2004).
  - [11] J. A. Chervenak and J. M. Valles, Jr., Phys. Rev. B **59**, 11209 (1999).
  - [12] J. M. Kosterlitz and D. J. Thouless, J. Phys. C **6**, 1181 (1973).
  - [13] M. R. Beasley, J. E. Mooij, and T. P. Orlando, Phys. Rev. Lett. **42**, 1165 (1979).
  - [14] A. F. Hebard and A. T. Fiory, Phys. Rev. Lett. **44**, 291 (1980).
  - [15] L. G. Aslamasov and A. I. Larkin, Phys. Lett. A **26**, 238 (1968).
  - [16] J. A. Chervenak and J. M. Valles, Jr., Phys. Rev. B **54**, R15649 (1996).
  - [17] D. J. Resnick, J. C. Garland, J. T. Boyd, S. Shoemaker, and R. S. Newrock, Phys. Rev. Lett. **47**, 1542 (1981).
  - [18] A. T. Fiory, A. F. Hebard, and S. Somekh, Apl. Phys. Lett. **32**, 73 (1978).
  - [19] G. S. Mkrtchyan and V. V. Shmidt, Soviet Phys. JETP **34**, 195 (1972).
  - [20] U. Welp, Z. Xiao, J. S. Jiang, et al., Phys. Rev. B **66**, 212507 (2002).
  - [21] A. Bezryadin and B. Pannetier, J. Low Temp. Phys. **98**, 251 (1995).
  - [22] From SEM images we have determined the hole lattice constant  $a = 100 \pm 5$  nm and thus  $H_M = 2390 \pm 240$  Gauss. The position of the peaks in the data occur at  $H = 2145 \pm 50$  Gauss in agreement with that calculated from the lattice con-

stant.  $H_M = 2145$  Gauss is the normalization used on the data throughout this paper.

- [23] A. J. Yin et al., Appl. Phys. Lett. **79**, 1039 (2001).
- [24] H. Masuda and K. Fukuda, Science **268**, 1466 (1995).
- [25] H. Masuda et al., Appl. Phys. Lett. **71**, 2770 (1997).
- [26] J. Li et al., Appl. Phys. Lett. **75**, 367 (1999).
- [27] X. S. Ling et al., Phys. Rev. Lett. **76**, 2989 (1996).
- [28] M. J. Higgins et al., Phys. Rev. B **61**, R894 (2000).
- [29] S. Teitel and C. Jayaprakash, Phys. Rev. Lett. **51**, 1999 (1983).
- [30] D. Belitz and T. R. Kirkpatrick, Rev. Mod. Phys. **66**, 261 (1994).
- [31] A. M. Finkelstein, Physica B **197**, 636 (1994).
- [32] B. Pannetier, J. Chaussy, and R. Rammal, J. Physique Lett. **44**, 853 (1983).
- [33] C. C. Abilio et al., J. Low Temp Phys. **118**, 23 (2000).
- [34] M. Hayashi and H. Ebisawa, Physica C **352**, 191 (2001).
- [35] T. R. Kirkpatrick and D. Belitz, Phys. Rev. Lett. **79**, 3042 (1997).
- [36] N. Goldenfeld, *Lectures on Phase Transitions and the Renormalization Group* (Addison-Wesley, New York, 1992).